DEVELOPMENTAL DYNAMICS 242:572–579, 2013

Characterization of *pax1*, *pax9*, and *uncx* Sclerotomal Genes During *Xenopus laevis* Embryogenesis

Romel Sebastián Sánchez and Sara S. Sánchez*

Background: The axial skeleton develops from the sclerotome, a mesenchymal cell population derived from somites. Sclerotomal cells migrate from somites to the perinotochordal and perineural space where they differentiate into chondrocytes to form cartilage and bone. In anurans, little is known about the way how the sclerotome changes as development proceeds and how these events are regulated at the molecular level. *Pax1*, *Pax9*, and *Uncx4.1* genes play a central role in the morphogenesis of the axial skeleton in vertebrates, regulating cell proliferation and chondrogenic specification of the sclerotome. Results: In this work, we cloned and examined through whole-mount *in situ* hybridization and reverse transcriptase-polymerase chain reaction the expression patterns of *pax1*, *pax9*, and *uncx* transcription factors in the anuran *Xenopus laevis*. Conclusions: We found that these genes are similarly expressed in the sclerotome and in the pharyngeal pouch. A detailed analysis of the location of these transcripts showed that they are expressed in different subdomains of the sclerotomal compartment and differ from that observed in other vertebrates. *Developmental Dynamics 242:572–579, 2013*. © 2013 Wiley Periodicals, Inc.

Key words: Anuran; *Xenopus*; Sclerotome; Backbone; *pax1*; *pax9*; *uncx*

Key findings:

- The *pax1*, *pax9*, and *uncx* genes of the anuran *Xenopus laevis* were cloned.
- The *pax1*, *pax9*, and *uncx* genes are expressed in the pharyngeal pouch and sclerotome in the tail bud stage of *Xenopus* embryos.
- The *pax1*, *pax9*, and *uncx* genes are expressed in different subdomains of the sclerotome of *Xenopus* embryos.

Accepted 31 January 2013

INTRODUCTION

The body of vertebrates is supported by the vertebral column, a series of segmental skeletal elements that provide both stability and mobility. Axial skeleton development is a multistep process which starts with the formation of somites from the unsegmented paraxial mesoderm that develop at both sides of the neural tube (Tam and Trainor, 1994; Christ and Ordahl, 1995). Shortly after formation, somites become compartmentalized into myotome, dermatome, and sclerotome. In the anuran *Xenopus laevis*, most somites are myotomal, consisting of cells that will form muscle while the dermatome, a small dorsal lateral part of the somite, will give rise to the dermis of the back, and the sclerotome will form the skeletal elements of the vertebral column and ribs (Keller, 2000).

The sclerotome, the smallest compartment of the somite, made up of polymorphic cells located at the somite ventromedial edge, is adjacent to the notochord, and only becomes distinct from the myotome after the tail bud stage (st. 30) (Youn and Malacinski, 1981a,b; Christ et al., 2004). Thereafter, these cells migrate from the somite to the perinotochordal and perineural space, where they proliferate and differentiate into cartilage

Departamento de Biología del Desarrollo, San Miguel de Tucumán, Argentina
Grant sponsor: Consejo Nacional de Investigaciones Científicas y Técnicas (CONICET); Grant sponsor: Agencia Nacional de Promoción Científica y Tecnológica (FONCYT); Grant sponsor: Consejo de Investigaciones de la Universidad Nacional de Tucumán (CIUNT).
***Correspondence to: Sara S. Sánchez, CONICET, UNT-INSIBIO, Departamento de Biología del Desarrollo, Chacabuco 461, San Miguel de Tucumán (T4000ILI), Argentina. E-mail: ssanchez@fbqf.unt.edu.ar**

DOI: 10.1002/dvdy.23945
Published online 9 February 2013 in Wiley Online Library (wileyonlinelibrary.com).

A

```
amphipax1 Branchiostoma   GEVNQLGGVFVNGRPLPNAIRLRIVELAQLGIRPCDISRQLRVSHGCVSKILARYNETGSILPGAIGGSK  78
pax1/9 Ptychodera         GEVNQLGGVFVNGRPLPNAIRLRIVELAQLGIRPCDISRQLRVSHGCVSKILARYNETGSILPGAIGGSK  79
pax1/9 Ciona              GEVNQLGGVFVNGRPLPNA RLRI IELAQLGIRPCDISRQLRVSHGCVSKILARYNETGSILPGAIGGSK 108
pax1 Xenopus              GEVNQLGGVFVNGRPLPNAIRLRIVELAQLGIRPCDISRQLRVSHGCVSKILARYNETGSILPGAIGGSK  75
pax1 Danio                GEVNQLGGVFVNGRPLPNAIR RIVELAQLGIRPCDISRQLRVSHGCVSKILARYNETGSILPGAIGGSK  77
pax1 Mus                  GEVNQLGGVFVNGRPLPNAIRLRIVELAQLGIRPCDISRQLRVSHGCVSKILARYNETGSILPGAIGGSK  75
pax1 Homo                 GEVNQLGGVFVNGRPLPNAIRLRIVELAQLGIRPCDISRQLRVSHGCVSKILARYNETGSILPGAIGGSK 169
pax1 Gallus               GEVNQLGGVFVNGRPLPNAIRLRIVELAQLGIRPCDISRQLRVSHGCVSKILARYNETGSILPGAIGGSK  74
pax9 Homo                 GEVNQLGGVFVNGRPLPNAIRLRIVELAQLGIRPCDISRQLRVSHGCVSKILARYNETGSILPGAIGGSK  75
pax9 Mus                  GEVNQLGGVFVNGRPLPNAIRLRIVELAQLGIRPCDISRQLRVSHGCVSKILARYNETGSILPGAIGGSK  75
pax9 Xenopus              GEVNQLGGVFVNGRPLPNAIRLRIVELAQLGIRPCDISRQLRVSHGCVSKILARYNETGSILPGAIGGSK  75
pax9 Gallus               GEVNQLGGVFVNGRPLP AIRLRIVELAQLGIRTCDISRQLRFSHGCVSKILARYNETGSILPGAIGGSK  75
pax9 Danio                GEVNQLGGVFVNGRPLPNAIRLRIVELAQLGIRPCDISRQLRVSHGCVSKILARYNETGSILPGAIGGSK  75

amphipax1 Branchiostoma   PRVTTPEVVKAIKKYKTLDPGIFAWEIRDRLLA GVCDKYNVPSVSSISRILRNKIG  135
pax1/9 Ptychodera         PRVTTPTVVNHIKEYKQHDPGIFAWEIRDRL ADGVCDKYNVPSVSSISRILRNKIG  136
pax1/9 Ciona              PRVTTPGVVNAIKDYKVRDPGIFAWEIRDRLL SDAVCDKYNVPSVSSISRILRNKIG  165
pax1 Xenopus              PRVTTPTVVKHIRDYKQGDPGIFAWEIRDRLLAD NVCDKYNVPSVSSISRILRNKIG  132
pax1 Danio                PRVTTPNVVKSIRDYKQGDPGIFAWEIRDRLLADGVCDKYNVPSVSSISRILRNKIG  134
pax1 Mus                  PRVTTPNVVKHIRDYKQGDPGIFAWEIRDRLLADGVCDKYNVPSVSSISRILRNKIG  132
pax1 Homo                 PRVTTPNVVKHIRDYKQGDPGIFAWEIRDRLLADGVCDKYNVPSVSSISRILRNKIG  226
pax1 Gallus               PRVTTPNVVKHIRDYKQGDPGIFAWEIRDRLLADGVCDKYNVPSVSSISRILRNKIG  131
pax9 Homo                 PRVTTPTVVKHIRTYKQRDPGIFAWEIRDRLLADGVCDKYNVPSVSSISRILRNKIG  132
pax9 Mus                  PRVTTPTVVKHIRTYKQRDPGIFAWEIRDRLLADGVCDKYNVPSVSSISRILRNKIG  132
pax9 Xenopus              PRVTTPTVVKHIRTYKQRDPGIFAWEIRDRLLADGVCDKYNVPSVSSISRILRNKIG  132
pax9 Gallus               PRVTTPTVVKHIRTYKQRDPGIFAWEIRDRLLADGVCDKYNVPSVSSISRILRNKIG  132
pax9 Danio                PRVTTPNVVKHIRTYKQRDPGIFAWEIRDRLLADGVCDK NVPSVSSISRILRNKIG  132
```

B

```
amphipax1 Branchiostoma   HTVSDILG  202
pax1/9 Ptychodera         HSVNDILG  198
pax1/9 Ciona              HSVTEILR  244

pax1 Xenopus              HSVNNILG  204
pax1 Danio                HTVSNILG  197
pax1 Mus                  HSVSNILG  203
pax1 Homo                 HSVSNILG  297
pax1 Gallus               HSVTNILG  203

pax9 Homo                 HSVTDILG  203
pax9 Mus                  HSVTDILG  203
pax9 Xenopus              HSVTDILG  201
pax9 Gallus               HSVTDILG  203
pax9 Danio                HSVTDILG  204
```

C

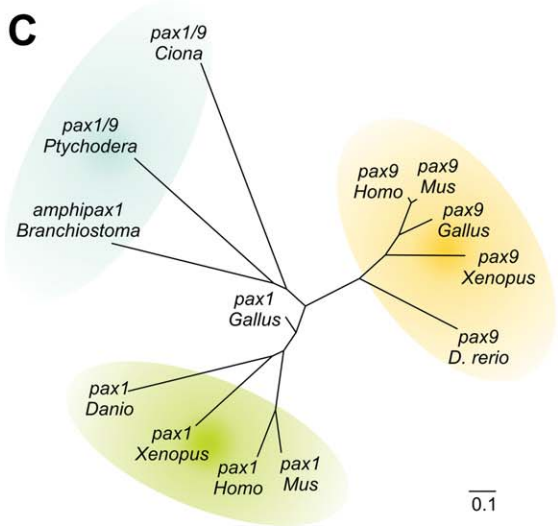

Fig. 1. Analysis of Pax1 and Pax9 protein sequences. **A:** Amino acid sequence comparison of the paired-box domain between *Xenopus laevis* Pax1 and Pax9 and their orthologues in other species. Identical amino acids are black, conserved changes are gray, changes not conserved are red, and the variable amino acids are green. The absence of residues at the corresponding region is indicated by dashes. **B:** Amino acid sequence comparison of the octapeptide between *X. laevis* Pax1 and Pax9 and their orthologues in other species. **C:** Molecular phylogenetic analysis of *X. laevis* Pax1 and Pax9 shows the relationship with their orthologues in other species. The protein sequences of different Pax1 and Pax9 protein were analyzed using ClustalW 2.1, and an unrooted tree was constructed by neighbor-joining analysis. The Pax1 and Pax9 protein sequences used were: *X. laevis* (AFN10837.1 and AFN10838), *Branchiostoma lanceolatum* (CAB42656.1), *Ciona intestinalis* (NP_001027594.1), *Ptychodera flava* (BAA78380.1), *Danio rerio* (CAQ15854.1 and NP_571373.1), *Gallus gallus* (AAA65058.1 and Uniprot: F1N8X4), *Mus musculus* (AAK01146.1 and NP_035171.1) and *Homo sapiens* (NP_006183.2 and CAB41533.1).

and bone of the vertebrae and intervertebral discs (Mookerjee, 1931). In anurans, the vertebral column diverges widely from that of other vertebrates and is characterized by a reduction in the number of vertebrae, absence of discrete caudal vertebrae, and a truncated axial skeleton (Handrigan and Wassersug, 2007). This divergent morphology emerges as a product of the evolutionary modulation of the generalized vertebrate developmental machinery. The acquisition of these morphological features could be associated with changes in the expression patterns and/or functional diversification of the genes involved in the regulation of the proliferation and differentiation of the sclerotome (Handrigan and Wassersug, 2007). Nevertheless, little is known about the way in which the sclerotomal cells change as

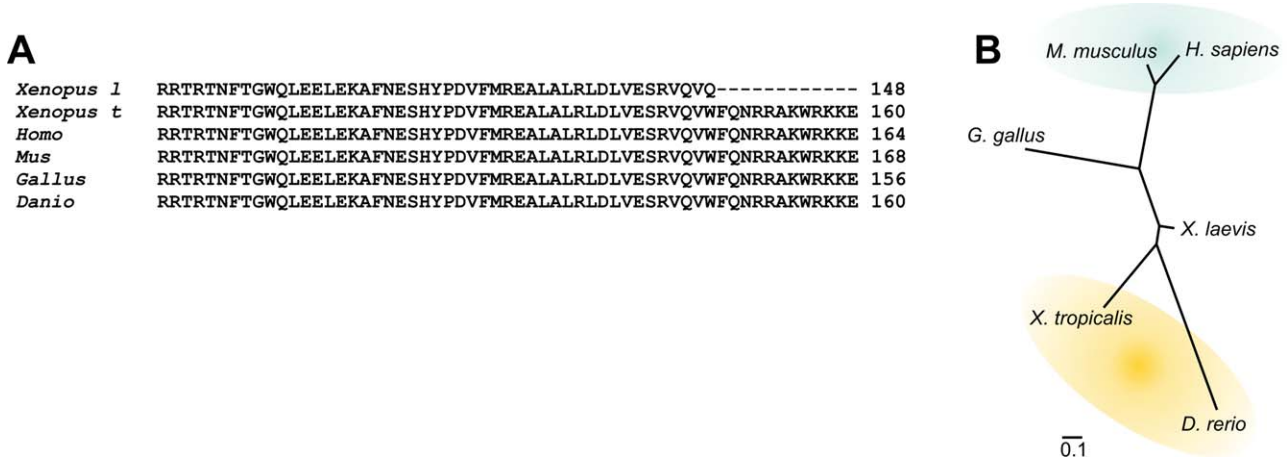

Fig. 2. Analysis of Uncx4.1 protein sequences. **A:** Amino acid sequence comparison of the homeobox domain between *Xenopus laevis* Uncx and its orthologues in other species. Identical amino acids are black. The absence of residues at the corresponding region is indicated by dashes. **B:** Molecular phylogenetic analysis of *X. laevis uncx* shows the relationship with its orthologues in other species. The protein sequences of different Uncx4.1 protein were analyzed using ClustalW 2.1, and an unrooted tree was constructed by neighbor-joining analysis. The Uncx4.1 protein sequences used were: *X. laevis* (AFN10839), *X. tropicalis* (Uniprot: F6ZJQ2), *D. rerio* (AAX73253.1), *G. gallus* (Uniprot: F1N8X4), *M. musculus* (CAB09537.1), and *H. sapiens* (NP_001073930.1).

development proceeds and how these events are regulated at the molecular level in *Xenopus laevis* (Keller, 2000).

Pax1 and Pax9 play an important role in the formation of the vertebrate axial skeleton, regulating cell proliferation and chondrogenic specification in the sclerotome (Wallin et al., 1994; Peters et al., 1999; Rodrigo et al., 2003). They belong to the Pax family of transcription factors, characterized by the presence of the paired-box domain and of the octapeptide sequence that interacts with the *Groucho* corepressor and by the absence of a homeobox domain (Strachan and Read, 1994; Eberhard et al., 2000). Both genes are derived from an ancestral preduplication *Pax1/9* gene present in ascidians and amphioxus (Holland et al., 1995). While *Pax1/9* is expressed only in the endoderm of the developing pharynx (Holland et al., 1995; Ogasawara et al., 1999; Hetzer-Egger et al., 2000), *Pax1* and *Pax9* have an additional expression in the sclerotomal cells of vertebrates (Wallin et al., 1994; Neubuser et al., 1995; Muller et al., 1996; Nornes et al., 1996; Mise et al., 2008). The functional importance of Pax genes for vertebrate development is demonstrated by the defects of several classical mouse and human mutations (reviewed by Tremblay and Gruss, 1994). After *Pax1/9* was duplicated into *Pax1* and *Pax9*, their roles were subfunctionalized as evolution progressed. In medaka fish, *Pax1* and *Pax9* showed similar expression patterns, except for a strong expression of *Pax9* in mesodermal cells of the tail bud that was not observed for *Pax1* (Mise et al., 2008). In chicken and mouse, *Pax1* and *Pax9* exhibited more significant differences in their expression patterns: while *Pax9* is expressed mainly in the dorsolateral regions of the sclerotome, *Pax1* is expressed in the ventromedial region of the mouse sclerotome and in almost all cells of the chicken sclerotome (Muller et al., 1996; Neubuser et al., 1995). Subfunctionalization of *Pax1* and *Pax9* roles was supported by the functional studies performed in fish and mouse, where regionalization of their expressions in the sclerotome was found to regulate the differentiation of the distinct components of the vertebrae (Peters et al., 1998, 1999; Wilm et al., 1998; Mise et al., 2008).

Another gene involved in the development of the axial skeleton is *Uncx4.1*. This gene encodes a paired-type homeobox transcription factor expressed in the developing somite and sclerotome (Saito et al., 1996; Mansouri et al., 1997). In mouse, it is first expressed in the entire caudal half of the newly formed somite and later only in the sclerotome (Mansouri et al., 1997). Additionally, functional studies have shown that *Uncx4.1* is required for the condensation of mesenchymal cells of the

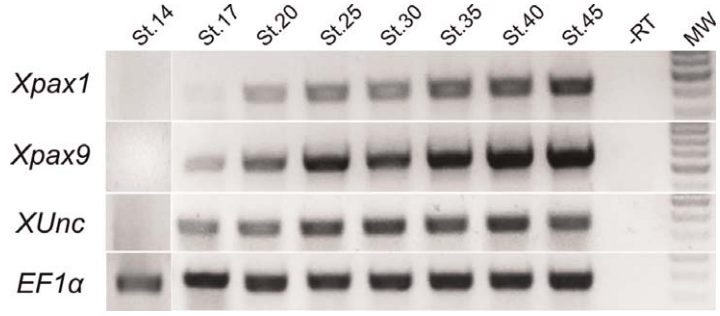

Fig. 3. Temporal expression pattern of *Xenopus pax1*, *pax9*, and *uncx* by reverse transcriptase-polymerase chain reaction (RT-PCR) analysis. RT-PCR was performed with total RNA from different developmental stages. The negative control was performed omitting reverse transcriptase enzyme in reaction (−RT). *EF1α* served as a loading control. The last lane corresponds to the molecular weight marker (MW).

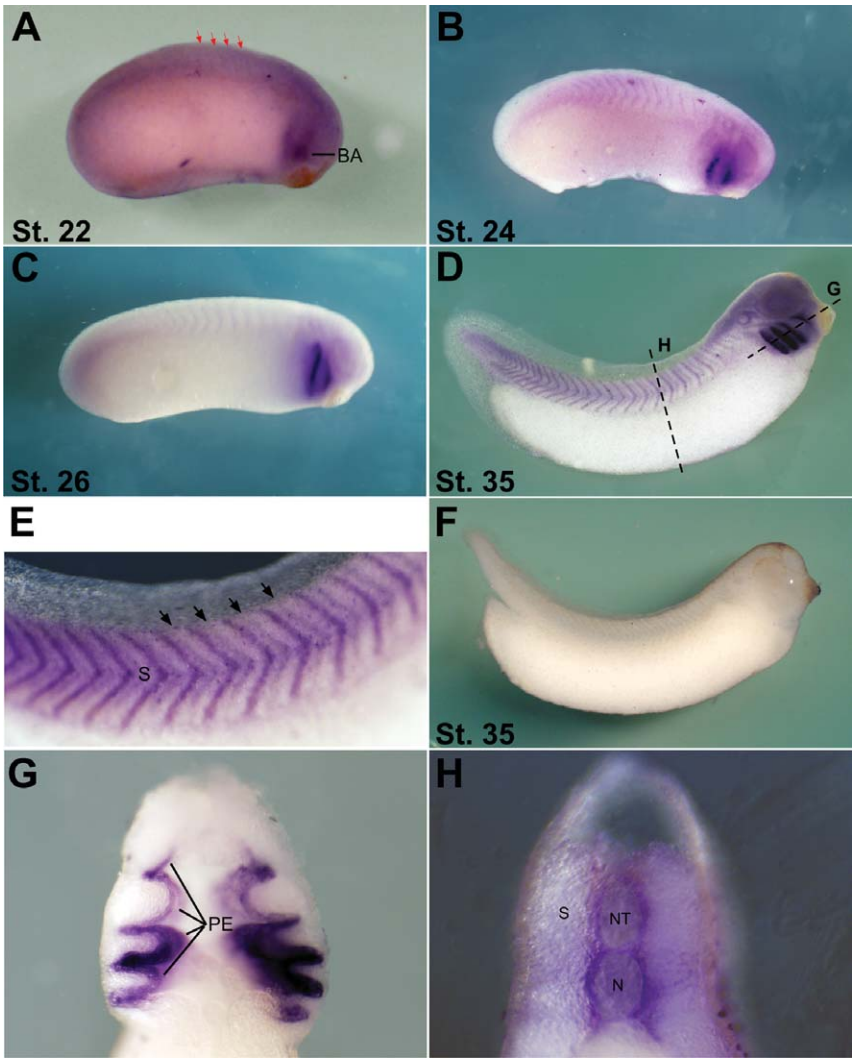

Fig. 4. Spatial expression of *pax1* transcripts during *Xenopus* development. Whole-mount *in situ* hybridization was carried out using a digoxigenin-labeled riboprobe. A–F: Lateral view, anterior is to the right. **A:** At stage 22, *pax1* is expressed in the branchial arches and weakly in the somite (red arrows). **B–D:** The *pax1* expression is increased and its localization advances progressively to caudal region of the somites in the stage 24 (B), stage 26 (C), and stage 35 embryos (D). **E:** Magnification of the dorsal region of D at the somite level. Black arrows indicate the intersomitic space. **F:** Whole-mount *in situ* hybridization with *pax1* sense probe was used as negative control. **G,H:** Transverse sections of stage 35 embryos at the branchial arches level (G) and trunk (H). Nieuwenkoop-Faber stages are indicated on the lower left corner. BA, branchial arches; N, notochord; NT, neural tube; PE, pharyngeal endoderm; S, somite.

lateral sclerotome, which is necessary for the specification of pedicles, transverse processes, and proximal ribs (Leitges et al., 2000; Mansouri et al., 2000).

In this study, we isolated the full-length cDNAs of *pax1*, *pax9*, and *uncx* (orthologue of *Uncx4.1*) of *Xenopus laevis* and characterized their expression profiles in the developing *Xenopus* embryo by whole-mount *in situ* hybridization and reverse transcriptase-polymerase chain reaction (RT-PCR) assay. We found that these three genes have similar but not identical expression patterns located in the sclerotome and in the endoderm of the pharyngeal pouch during *Xenopus laevis* development.

RESULTS AND DISCUSSION

Isolation and Characterization of *Xenopus pax1*, *pax9*, and *uncx* cDNA

The clones of *pax1*, *pax9*, and *uncx* transcription factors were identified in a screening of an *X. laevis* expressed sequence tag (EST) library. Sequence analysis of *pax1*, *pax9* and *uncx* cDNA revealed that they contain an open reading frame of 1077, 1083, and 492 nucleotides that encode proteins predicted to be of 358, 361 and 164 amino acids respectively (GenBank accession no. JQ929179, JQ929180, and JQ929181).

Comparison of the deduced amino acid sequence of *Xenopus* Pax1 with chick, human, mouse, and zebrafish Pax1 proteins revealed 83, 76, 74, and 71% sequence identity respectively, while the comparison of the deduced amino acid sequence for *Xenopus* Pax9 with its orthologue in these organisms showed a value of 91, 83, 83, and 70% sequence identity, respectively.

Previous studies have shown that *Pax1* and *Pax9* genes derive from an ancestral *Pax1/9* gene (Holland et al., 1995). This phylogenetic relationship is reflected in the homology between Pax1 and Pax9 *Xenopus* proteins, which show 71% sequence identity.

An unrooted phylogenetic tree including Pax1 and Pax9 as well as the ancestral Pax1/9 protein sequences clearly indicates the close relationship between these proteins, where Pax1 and Pax9 were grouped with their orthologues (Fig. 1C).

The comparison of the paired-box domain and octapeptide sequences of vertebrates Pax1 and Pax9, and the ancestral Pax1/9 protein of Hemichordata (*Ptychodera flava*), Urochordata (*Ciona intestinalis*), and Cephalochordata (*Branchiostoma lanceolatum*) revealed a striking conservation of the these domains (Fig. 1A,B). It is interesting to note that this gene has remained almost invariable for more than 500 million years, since the divergence between hemichordata and vertebrate lineages (Blair and Hedges, 2005). However, the comparison of the C-terminal region where the transactivation domain is located presented low homology between Pax1 and Pax9 proteins. This could be related to the fact that the C-terminal region undergoes alternative splicing, leading to functionally distinct *Pax1* and *Pax9* genes (Short and Holland, 2008).

The comparison of the deduced amino acid sequence of *Xenopus* Uncx

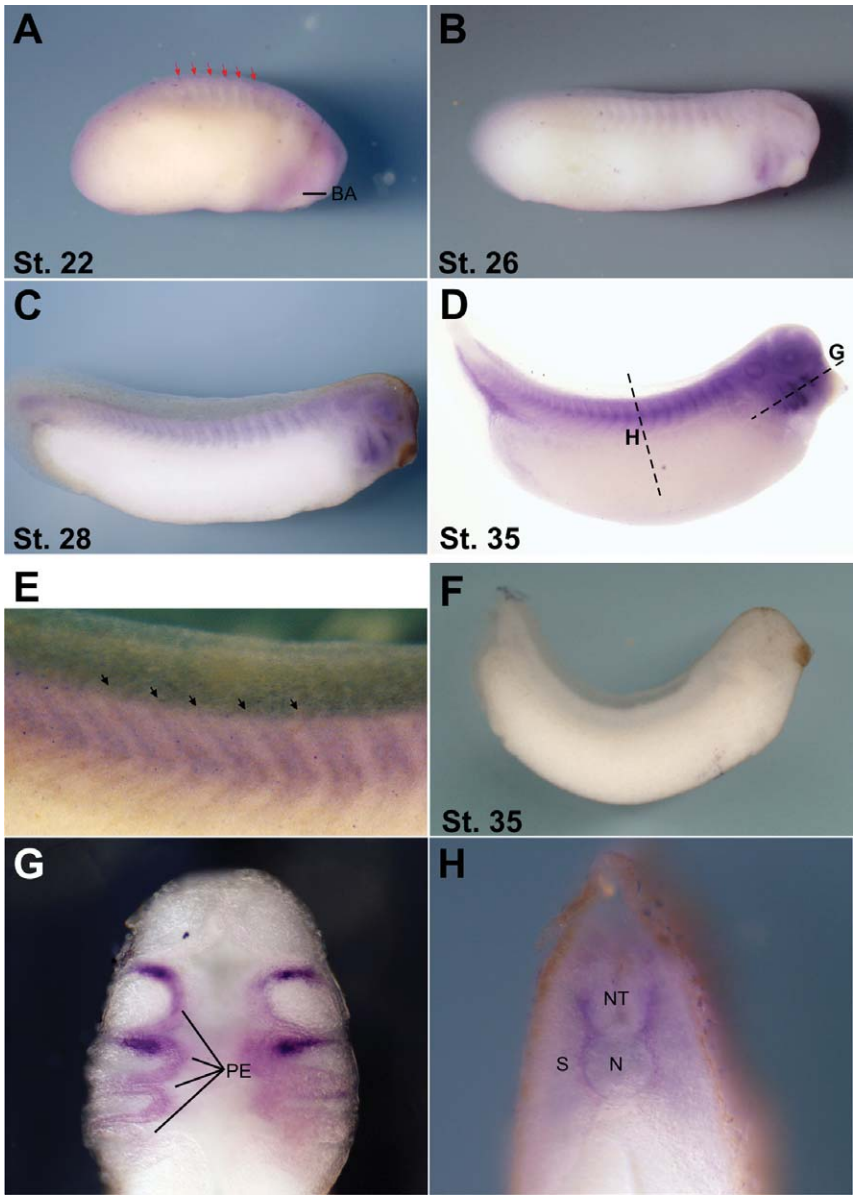

Fig. 5. Spatial expression of *pax9* transcripts during *Xenopus* development. Whole-mount *pax9 in situ* hybridization. A–F: Lateral view, anterior is to the right. **A:** At stage 22, *pax9* is weakly expressed in the branchial arches and in the somite (red arrows). **B–D:** *pax9* expression is increased and its localization advances progressively to caudal region in the stage 26 (B), stage 28 (C), and stage 35 embryos (D). **E:** Magnification of the dorsal region of C at the somites level. Black arrows indicate the intersomitic space. **F:** Whole-mount *in situ* hybridization with *pax9* sense probe. **G,H:** Transverse sections of stage 35 embryos at the branchial arches level (G) and trunk (H).

with *Xenopus tropicalis*, human, mouse, chick, and zebrafish Uncx4.1 protein reveals 95, 85, 85, 85, 83% sequence identity, respectively. Alignment of Uncx4.1 protein sequences from different species shows that the homeodomain region is highly conserved (Fig. 2A). A phylogenetic tree based on amino acid sequences indicated that the Uncx4.1 orthologues of zebrafish and *X. tropicalis* form a group distinct from mammalian, while *X. laevis* is widely distant from both groups (Fig. 2B). The sequence of the *X. laevis* Uncx protein is much smaller than that in other organisms, including *X. tropicalis*. Although we performed an exhaustive search in different gene databases of *X. laevis*, we were unable to find isoforms of this gene. Consequently, we cannot conclude if this difference observed in the size of the protein corresponds to an isoform or is characteristic of the *uncx* gene in *Xenopus laevis*.

Temporal Expression of *pax1*, *pax9*, and *uncx*

The temporal expression of *pax1*, *pax9*, and *uncx* was analyzed by reverse transcriptase-polymerase chain reaction (RT-PCR) using total RNAs isolated from different developmental stages of *Xenopus laevis* embryos (Fig. 3). The expression of these genes begins during early somitogenesis (st. 17). The transcripts were most abundant during the tail bud stage (st. 25) and expression continued throughout the tadpole stage (st. 30–35-45), suggesting that in *X. laevis pax1*, *pax9*, and *uncx* may be required not only for the differentiation of sclerotomal cells but also for the initiation and maintenance of sclerotome development.

Spatial Expression of *pax1*, *pax9*, and *uncx*

We examined the spatial distribution of *Xenopus pax1*, *pax9*, and *uncx* transcripts by whole-mount *in situ* hybridization and subsequent histological analyses. The three genes showed similar but not identical expression patterns. The expression of *pax1*, *pax9*, and *uncx* was detected from early tail bud stage in the branchial arches and somites around stage 21–22 (Figs. 4A, 5A, 6A). However, the expression of *uncx* in somitic region was observed later (Fig. 6B). As development continues, the expression of these genes in the somites progressed from rostral to caudal direction (Figs. 4B–D, 5B–D, 6B–D). These transcripts are expressed in a similar way in the newly formed branchial arches. Histological examination of late tail bud stage embryos (st. 35) enabled a more detailed analysis of the location of the transcripts. Transverse sections of somite and pharyngeal pouch showed that the expression of *pax1*, *pax9*, and *uncx* is located in the sclerotome and endodermal pharyngeal pouch (Figs. 4G,H, 5G,H, 6G,H), as reported for other vertebrates (Neubuser et al., 1995; Peters et al., 1995; Saito et al., 1996; Mansouri et al., 1997; Mise et al., 2008). In this study

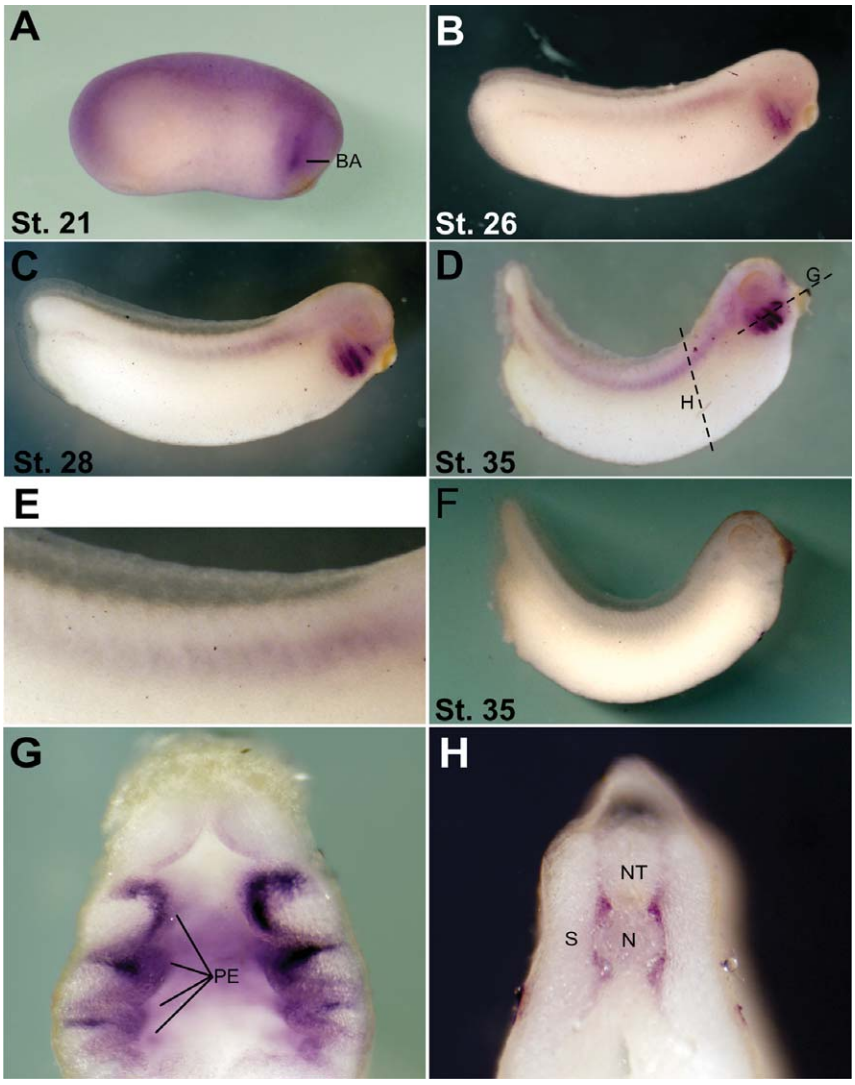

Fig. 6. Spatial expression of *uncx* transcripts during *Xenopus* development. Whole-mount *uncx in situ* hybridization. A–F: Lateral view, anterior is to the right. **A:** At stage 21, *uncx* is weakly expressed in the branchial arches. **B:** At stage 26, *uncx* is strongly expressed in the branchial arches and in the anterior somitic region. **C,D:** Expression *uncx* in the in stage 28 (C) and stage 35 (D). **E:** Magnification of the dorsal region of C at the somites level. **F:** Whole-mount *in situ* hybridization with *pax9* sense probe. **G,H:** Transverse sections of stage 35 embryos at the branchial arches level (G in panel D) and trunk (H in panel D).

we detected differences between the spatial expression pattern of *Xenopus pax1* and *pax9*, which in turn differs from the pattern of their orthologues observed in other vertebrates. In fish, the expression of *pax1* and *pax9* mRNA in the sclerotome is restricted to the ventromedial region of the somite and no differences were detected in their spatial patterns (Mise et al., 2008). However, in amniotes, *Pax1* and *Pax9* subfunctionalized their roles in the development of the sclerotome (Mise et al., 2008). In mice, while *Pax9* is mainly expressed in the lateral region of the sclerotome, *Pax1* is expressed medially and ventromedially (Deutsch et al., 1988; Neubuser et al., 1995). Similarly, in chicken, *PAX1* is expressed in almost all sclerotome cells, whereas *PAX9* expression is found mainly in dorsolaterally located sclerotomal cells (Muller et al., 1996). In the anuran *Xenopus laevis*, we found that the expression of *pax1* is located in the sclerotomal cells of the center of the somites surrounding the notochord and neural tube (Fig. 4E,G,H), whereas *pax9* is expressed mainly in the anterior half of the sclerotome around the neural tube (Fig. 5C,E). These sublocations of *pax1* and *pax9* in the sclerotome could be involved in the regionalization of the sclerotome and in the differentiation of the vertebral column components.

For *Xenopus uncx* factor, we observed that it is expressed only in the sclerotomal cells surrounding the notochord (Fig. 6E,G,H). This sublocalization in the sclerotome differs from the one observed in mouse, in which *Uncx4.1* is expressed in the entire caudal half of the sclerotome (Mansouri et al., 1997). To the best of our knowledge, in other orders of vertebrates the expression pattern of *Uncx4.1* has not been described yet.

Pax1, *Pax9*, and *Uncx4.1* genes play a central role in the formation of the axial skeleton of vertebrates. As in other vertebrates, the expression of *pax1*, *pax9*, and *uncx* genes in *Xenopus* was subregionalized within the sclerotome, so that they would possibly regulate the formation of different components of the vertebral column. The spatial expression pattern of these genes in *Xenopus* differs from those observed in other vertebrate models, which would make them at least partly responsible for the divergent morphogenesis of the vertebral column in anurans.

EXPERIMENTAL PROCEDURES

Identification and Isolation of cDNA Clones

The NCBI database was screened by using high stringency Tblastx against a pool of *Xenopus laevis* ESTs from different *Xenopus laevis* embryonic libraries. The sequences of the *Pax1*, *Pax9*, and *Uncx4.1* mRNA from mouse (GenBank accession no. NM_008780, NM_011041 and BC051973) were used as probes, and we identified several interesting ESTs. The clones XL085n23 (kindly provided by Dr. Naoto Ueno, NIBB, Okazaki, Japan), BC084222, and BC044278 (acquired through the IMAGE Consortium/LLNL) were fully sequenced, with an open reading frame encoding for *X. laevis pax1*, *pax9*, and *uncx* protein, respectively. Alignments of amino acid sequences were done using the ClustalW algorithm (http://www.ebi.ac.uk/Tools/msa/clustalw2/).

The phylogenetic tree was drawn using the Phylodendron application (http://iubio.bio.indiana.edu/treeapp/treeprintform.html).

Embryo Manipulation

Adult male and female *Xenopus laevis* specimens were stimulated with 400 IU and 800 IU of human chorionic gonadotropin (HCG –Elea Lab.), respectively. Fertilized eggs were obtained after natural single-pair mating and they were dejellied with 2% cysteine hydrochloride (pH 7.8) and cultured in 1× NAM. They were staged according to the Nieuwkoop and Faber tables (1967).

RNA Isolation and RT-PCR Expression Analysis

Total RNA was isolated from whole embryos using TRIREAGENT reagent (MRC) according to manufacturer's instructions. cDNAs were synthesized by M-MLV reverse transcriptase (Promega) with oligo(dT^{15}) priming from 1 μg total RNA extracted from embryos at different stages. PCRs were performed with GoTaq polymerase (Promega) in semiquantitative amplification conditions and *EF-1α* was used as an internal standard. The oligonucleotide primers and cycling conditions designed for this study were: *EF-1α*, 5′-CAG ATT GGT GCT GGA TAT GC-3′ and 5′-ACT GCC TTG ATG ACT CCT AG-3′, 25 cycles; *pax1*, 5′-CTA CCC TAC CAG CAA CCA ATA TG-3′ and 5′-CAA CTG TCC CAC TAA ATC ACC TC-3′, 29 cycles; *pax9*, 5′-AGT AGG AAC ACG TTT CAG TCG-3′ and 5′-TTG GAT CCT AGA GAT GAC AGC-3′, 30 cycles; *uncx*, 5′-TTA AGA CCC TGG AGG TGT GG-3′ and 5′-TGT TTT CGC CCC TGT AAT TC-3′, 30 cycles. The PCR products were analyzed on 1.5% agarose gels. As a negative control, PCR was performed with RNA that had not been reverse-transcribed to check for DNA contamination.

Whole-Mount *In Situ* Hybridization

The embryos fixation and whole-mount *in situ* hybridization with digoxigenin-UTP RNA probes were carried out as previously described by Harland (1991), with minor modifications as described by Mancilla and Mayor (1996) and Monsoro-Burq (2007). Antisense RNA probes for *pax1*, *pax9*, and *uncx* were transcribed with T7 RNA polymerase from *pax1*/pBluescript II, *pax9*/pCMV-sport6, and *uncx*/pCMV-sport6 templates linearized with *Eco*RV, *Bgl*II, and *Hin*dII, respectively. Digoxigenin-labeled sense probes were used as negative control. Sense probe for *pax1* was digested with *Apa*I and transcribed with T3 RNA polymerase, whereas the *pax9* and *uncx* probes were digested with *Bam*HI and *Pst*I, respectively, and transcribed with SP6 RNA polymerase. Detection of labeled probes was performed using alkaline-phosphatase conjugated anti-digoxigenin Fab fragments and with NBT/BCIP (nitroblue tetrazolium/5-bromo-4-chloro-3-indolyl phosphate) as substrate (Roche). Pigmented embryos were bleached with a solution containing 1% H_2O_2/PBS.

ACKNOWLEDGMENTS

We thank Naoto Ueno for the EST XL085n23 clone. This research was supported by Consejo Nacional de Investigaciones Científicas y Técnicas (CONICET) and CIUNT grants to S.S.S and Agencia Nacional de Promoción Científica y Tecnológica (FONCYT), Argentina. R.S.S. is a recipient of a CONICET (Argentina) Fellowship. S.S.S. is a Career Investigator of CONICET (Argentina). We also thank Ms. Virginia Mendez for her proofreading.

REFERENCES

Blair JE, Hedges SB. 2005. Molecular phylogeny and divergence times of deuterostome animals. Mol Biol Evol 22:2275–2284.

Christ B, Huang R, Scaal M. 2004. Formation and differentiation of the avian sclerotome. Anat Embryol (Berl) 208:333–350.

Christ B, Ordahl CP. 1995. Early stages of chick somite development. Anat Embryol (Berl) 191:381–396.

Deutsch U, Dressler GR, Gruss P. 1988. Pax 1, a member of a paired box homologous murine gene family, is expressed in segmented structures during development. Cell 53:617–625.

Eberhard D, Jimenez G, Heavey B, Busslinger M. 2000. Transcriptional repression by Pax5 (BSAP) through interaction with corepressors of the Groucho family. EMBO J 19:2292–2303.

Handrigan GR, Wassersug RJ. 2007. The anuran Bauplan: a review of the adaptive, developmental, and genetic underpinnings of frog and tadpole morphology. Biol Rev Camb Philos Soc 82:1–25.

Harland RM. 1991. In situ hybridization: an improved whole-mount method for Xenopus embryos. Methods Cell Biol 36:685–695.

Hetzer-Egger C, Schorpp M, Boehm T. 2000. Evolutionary conservation of gene structures of the Pax1/9 gene family. Biochim Biophys Acta 1492:517–521.

Holland ND, Holland LZ, Kozmik Z. 1995. An amphioxus Pax gene, AmphiPax-1, expressed in embryonic endoderm, but not in mesoderm: implications for the evolution of class I paired box genes. Mol Mar Biol Biotechnol 4:206–214.

Keller R. 2000. The origin and morphogenesis of amphibian somites. Curr Top Dev Biol 47:183–246.

Leitges M, Neidhardt L, Haenig B, Herrmann BG, Kispert A. 2000. The paired homeobox gene Uncx4.1 specifies pedicles, transverse processes and proximal ribs of the vertebral column. Development 127:2259–2267.

Mancilla A, Mayor R. 1996. Neural crest formation in Xenopus laevis: mechanisms of Xslug induction. Dev Biol 177:580–589.

Mansouri A, Voss AK, Thomas T, Yokota Y, Gruss P. 2000. Uncx4.1 is required for the formation of the pedicles and proximal ribs and acts upstream of Pax9. Development 127:2251–2258.

Mansouri A, Yokota Y, Wehr R, Copeland NG, Jenkins NA, Gruss P. 1997. Paired-related murine homeobox gene expressed in the developing sclerotome, kidney, and nervous system. Dev Dyn 210:53–65.

Mise T, Iijima M, Inohaya K, Kudo A, Wada H. 2008. Function of Pax1 and Pax9 in the sclerotome of medaka fish. Genesis 46:185–192.

Monsoro-Burq AH. 2007. A rapid protocol for whole-mount in situ hybridization on Xenopus embryos. CSH Protoc 2007:pdb prot4809.

Mookerjee HK. 1931. On the development of the vertebral column of anura. Philos Trans R Soc Lond 219:165–196.

Muller TS, Ebensperger C, Neubuser A, Koseki H, Balling R, Christ B, Wilting J. 1996. Expression of avian Pax1 and Pax9 is intrinsically regulated in the pharyngeal endoderm, but depends on environmental influences in the paraxial mesoderm. Dev Biol 178:403–417.

Neubuser A, Koseki H, Balling R. 1995. Characterization and developmental expression of Pax9, a paired-box-containing gene related to Pax1. Dev Biol 170:701–716.

Nieuwkoop PD, Faber J. 1967. Normal table of Xenopus laevis (Daudin). Amsterdam: North-Holland Publishing Co.

Nornes S, Mikkola I, Krauss S, Delghandi M, Perander M, Johansen T. 1996. Zebrafish Pax9 encodes two proteins with distinct C-terminal transactivating domains of different potency negatively regulated by adjacent N-terminal sequences. J Biol Chem 271:26914–26923.

Ogasawara M, Wada H, Peters H, Satoh N. 1999. Developmental expression of Pax1/9 genes in urochordate and hemichordate gills: insight into function and evolution of the pharyngeal epithelium. Development 126:2539–2550.

Peters H, Doll U, Niessing J. 1995. Differential expression of the chicken Pax-1 and Pax-9 gene: in situ hybridization and immunohistochemical analysis. Dev Dyn 203:1–16.

Peters H, Neubuser A, Balling R. 1998. Pax genes and organogenesis: Pax9 meets tooth development. Eur J Oral Sci 106(suppl 1):38–43.

Peters H, Wilm B, Sakai N, Imai K, Maas R, Balling R. 1999. Pax1 and Pax9 synergistically regulate vertebral column development. Development 126:5399–5408.

Rodrigo I, Hill RE, Balling R, Munsterberg A, Imai K. 2003. Pax1 and Pax9 activate Bapx1 to induce chondrogenic differentiation in the sclerotome. Development 130:473–482.

Saito T, Lo L, Anderson DJ, Mikoshiba K. 1996. Identification of novel paired homeodomain protein related to C. elegans unc-4 as a potential downstream target of MASH1. Dev Biol 180:143–155.

Short S, Holland LZ. 2008. The evolution of alternative splicing in the Pax family: the view from the Basal chordate amphioxus. Journal of molecular evolution 66:605–620.

Strachan T, Read AP. 1994. PAX genes. Curr Opin Genet Dev 4:427–438.

Tam PP, Trainor PA. 1994. Specification and segmentation of the paraxial mesoderm. Anat Embryol (Berl) 189:275–305.

Tremblay P, Gruss P. 1994. Pax: genes for mice and men. Pharmacol Ther 61:205–226.

Wallin J, Wilting J, Koseki H, Fritsch R, Christ B, Balling R. 1994. The role of Pax-1 in axial skeleton development. Development 120:1109–1121.

Wilm B, Dahl E, Peters H, Balling R, Imai K. 1998. Targeted disruption of Pax1 defines its null phenotype and proves haploinsufficiency. Proc Natl Acad Sci United States of America 95:8692–8697.

Youn BW, Malacinski GM. 1981a. Comparative analysis of amphibian somite morphogenesis: cell rearrangement patterns during rosette formation and myoblast fusion. J Embryol Exp Morphol 66:1–26.

Youn BW, Malacinski GM. 1981b. Somitogenesis in the amphibian Xenopus laevis: scanning electron microscopic analysis of intrasomitic cellular arrangements during somite rotation. J Embryol Exp Morphol 64:23–43.

Developmental Dynamics